Magnetic-field and temperature dependence of the photoinduced Faraday effect in diluted magnetic semiconductors

J. Frey, R. Frey, and C. Flytzanis
Laboratoire d'Optique Quantique du Centre National de la Recherche Scientifique, Ecole Polytechnique, 91128 Palaiseau CEDEX, France
(Received 22 July 1991)

The photoinduced Faraday process in the diluted magnetic semiconductor $Cd_{0.75}Mn_{0.25}Te$ is investigated for laser frequencies well below the semiconductor band gap. This study is performed through measurement of the giant photoinduced rotations of the laser polarization as the magnetic field, laser intensity, and temperature are changed. We identify three different contributions for the photoinduced Faraday rotation angle: a fast Kerr contribution proportional to the laser intensity, a population change due to two-photon absorption and carrier stimulated recombination, and a Mn^{2+}-ion magnetization as a consequence of the spin exchange interaction between the photocreated carriers and the magnetic ions. The last two contributions, which are quadratic in the laser intensity, saturate as the magnetic field increases, due to the saturation of the total spin of electrons and holes in the conduction and valence bands. An experimental study of the low-temperature dependence of the photoinduced Faraday rotation confirms the theoretical analysis and shows that the population and magnetic contributions are almost temperature independent while the Kerr term exhibits the same behavior as the linear Faraday rotation angle.

I. INTRODUCTION

The study of photoinduced variations of the propagation characteristics of a laser beam is of both fundamental and technological importance. Indeed, level shifts and population changes induced by intense short light pulses can lead to rapid modifications of either the refraction or absorption indices of a medium, which can give information about the nonlinear medium and lead to useful applications. Several aspects of these optical Kerr nonlinearities and their implications on the beam characteristics along its propagation direction have been extensively addressed in the literature.[1] In contrast, little has been done to exploit such light-mediated mechanisms to rapidly modify transverse characteristics of a beam. In a few isolated cases the photoinduced variation of the polarization state of the laser beam in the presence of a magnetic field has been observed: This has been done in metallic gases[2–4] and in intrinsic bulk II-VI semiconductors,[5] where only minute changes of the Faraday rotation angle were observed.

The situation however can be drastically different in the later case if the band electron states are appropriately modified through spin-exchange interaction with magnetic impurities which can act as "local amplifiers" of the magnetic field and induce giant Zeeman splittings of the dipole-allowed optical transitions;[6] this is precisely the origin of the giant Faraday polarization rotation observed[7] in diluted magnetic semiconductors (DMS) for light frequencies close to their band gap. Clearly, in the presence of an intense light beam the impact of these Zeeman splittings will be modified by level shifts and population changes and, through the amplifying effect of the spin-exchange interaction, we may expect giant light-induced modifications of the Faraday rotation as well; this was indeed recently demonstrated in $Cd_{1-x}Mn_xTe$, with $x=0.25$, where photoinduced modifications of several percents of the linear rotation angle were measured at room temperature for magnetic fields less than half a tesla.[8]

Here, we present an experimental and theoretical analysis which uses the magnetic-field, laser-intensity, and temperature dependence of the photoinduced Faraday rotation (PIFR) to delineate the physical origin of such a nonlinear rotation. In Sec. II we briefly describe the experimental setup and procedure. Section III is devoted to a detailed analysis of the temperature and magnetic-field dependence of the traditional Faraday rotation. In Sec. IV, we analyze the nonlinear phenomena (two-photon absorption and stimulated recombination of photoinduced free carriers) which are closely linked to the PIFR. The magnetic-field dependence of the photoinduced Faraday rotation is studied experimentally in Sec. V, which also contains a theoretical approach to PIFR and a discussion to compare theoretical and experimental results. Finally, Sec. VI shows that the temperature dependence of the PIFR is also in good agreement with the theoretical analysis of Sec. V.

II. EXPERIMENTAL SETUP AND PROCEDURE

In our experiment, the polarization rotation angle was measured by means of an analyzer as a function of several parameters: light intensity, magnetic-field amplitude, and temperature. The experimental setup and data-gathering procedure were cursorily described in Refs. 8 and 9. The main change in the latest case was the introduction of the DMS sample in a cryomagnetic system which allowed a controlled temperature variation in the range 4–300 K. However, results presented in this paper were obtained at low temperature ($T<20$ K). A small Faraday rotation (0.6° per T) was measured with no sample, which was due

to the silica windows of the cryostat. This rotation was temperature independent and had no photoinduced contribution. As a consequence, it did not influence the photoinduced Faraday rotations, which were obtained by making the difference between the polarization directions for high and low laser intensities, respectively.

Let us also recall that the light pulses, 35 ps in duration, delivered from a transverse monomode-mode locked Nd-YAG laser, were focused onto the $Cd_{0.75}Mn_{0.25}Te$ with a band gap at 1.95 eV, well above the laser frequency (1.16 eV), so that the medium was one-photon transparent at the laser frequency, and the conduction-band states could only be reached and populated by two-photon transitions.

III. LINEAR FARADAY ROTATION

The linear Faraday rotation was observed at low laser intensity at a temperature of 10 K. Figure 1 shows the Faraday rotation angle θ_L as a function of the magnetic field H. As expected, θ_L is almost proportional to H, a small saturation (4% at 3 T) occurring only for magnetic fields larger than 2T. As demonstrated by several authors[7,10,11] the Faraday effect in DMS is due to the spin-exchange interaction between band electrons and the d electrons of the Mn^{2+} ions.[6] The polarization rotation θ_L associated with this Faraday effect is, therefore, proportional to the magnetization of the paramagnetic Mn^{2+} ions.

At low temperature ($T<20$ K) Gaj, Planel, and Fishmen[12] derived an expression of the magnetization M_0 of

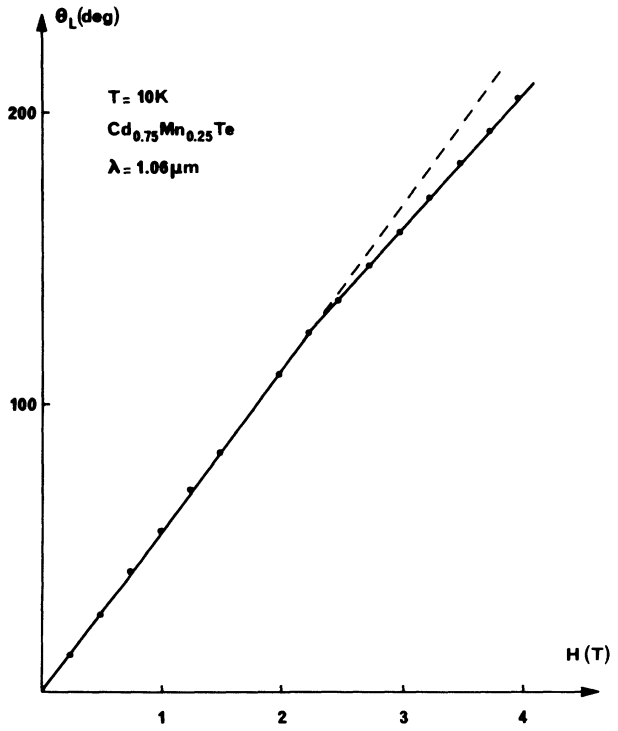

FIG. 1. Linear Faraday rotation angle as a function of the magnetic field.

Mn^{2+} ions induced by the magnetic field H in terms of an effective Brillouin function

$$M_0=\bar{x}N_0\, g_{\mathrm{Mn}}\mu_B J B_J(g_{\mathrm{Mn}}J\mu_B H/k_B(T+T_{AF})) \quad (1)$$

where N_0 is the number of cations per unit volume, $g_{\mathrm{Mn}}\approx 2$ the Landé factor for the Mn^{2+} ion, μ_B the Bohr magneton, and k_B the Boltzmann constant. B_J is the standard Brillouin function for $J=\frac{5}{2}$ in the case of Mn^{2+} ions. Finally, $\bar{x}$ and T_{AF} are empirical coefficients which represent an effective manganese concentration and an antiferromagnetic temperature, respectively. Both $\bar{x}$ and T_{AF} were shown to be dependent on the concentration x of Mn^{2+} ions.[7,12]

If H is small enough, which is the case for magnetic fields smaller than 3 T (see Fig. 1), the Brillouin function can be reduced to its argument so that M_0 can be written

$$M_0=\frac{\bar{x}AH}{T+T_{AF}}\ , \quad (2)$$

where $A=N_0(g_{\mathrm{Mn}}\mu_B)^2J(J+1)/3k_B$. Consequently, the linear Faraday rotation angle θ_L is given by

$$\theta_L=\frac{mH}{T+T_{AF}}\ , \quad (3)$$

where m is a constant which is proportional to $\bar{x}A$ and depends on the laser frequency.

Due to Eqs. (2) and (3), θ_L can be used to monitor the magnetization. Indeed, this technique was already used to determine the temperature dependence of the Verdet constant $m/(T+T_{AF})$ in Cd-Mn-Te.[7] The procedure used in Ref. 7 consisted of measuring θ_L vs H at a given temperature and plotting the inverse of the Verdet constant versus the temperature, thus allowing one to give the dependence of m and T_{AF} on the Mn^{2+} ion concentration. However, such a technique does not allow a determination of the exact dependence of θ_L (or equivalently M_0) with respect to H at a given temperature. Such a dependence could be found by measuring θ_L as a function of T for a given magnetic field. Results are presented in Fig. 2, which shows θ_L^{-1} vs T for $H=0.5$, 1, and 2 T. The linear dependence versus T is quite good for temperatures between 6 and 15 K. For temperatures larger than 20 K we observed a saturation of θ_L, while below 6 K, a cusp could be seen which corresponded to the paramagnetic spin glass phase transition.[13] From Fig. 2 it can be easily seen that the value of the intercept T_{AF} on the T axis depends on the magnetic field. This value T_{AF} is plotted in Fig. 3 as a function of H together with the Verdet constant m extracted from the slope of the straight lines of Fig. 2. A linear dependence of both T_{AF} and m can be, therefore, supposed for these two phenomenological constants. Note that T_{AF} varies by a factor larger than 3 for magnetic fields smaller than 3 T. This large variation, together with the growth of m for increasing magnetic fields, suggests that the coupling between Mn^{2+} ions becomes more efficient at larger magnetic fields.

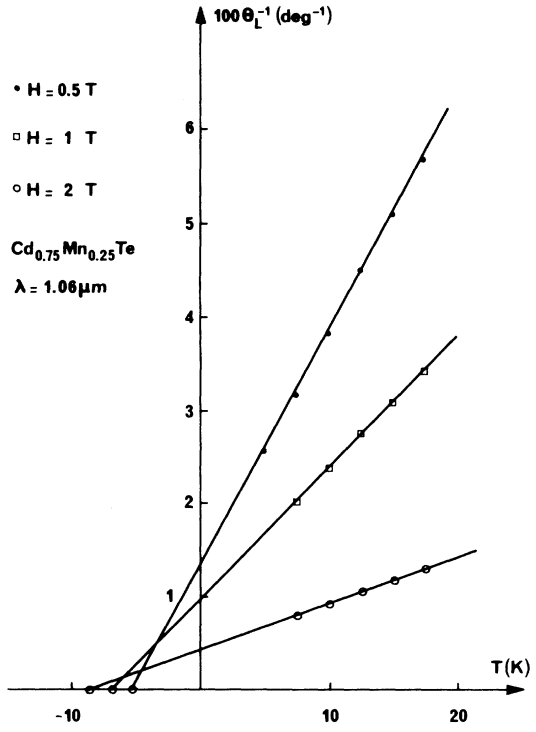

FIG. 2. Inverse of the linear Faraday rotation angle as a function of the temperature for different values of the magnetic field. Note that the intercepts of the T axis by the fits differ from each other.

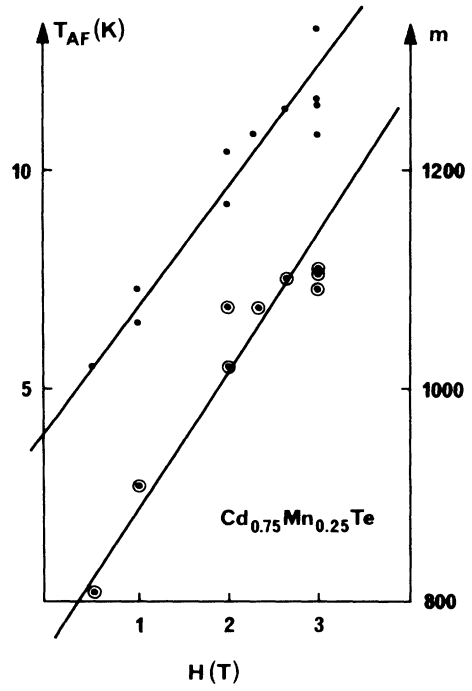

FIG. 3. Antiferromagnetic temperature (T_{AF}) and Verdet constant (m) as a function of the magnetic field.

IV. NONLINEAR PHENOMENA RELATED TO PIFR

Before turning our attention to the photoinduced Faraday rotation, it is useful to describe the nonlinear phenomena (two-photon absorption and stimulated recombination of free carriers) which may play an important role in this nonlinear magneto-optical process. Indeed, due to the high laser intensity, free carriers are created by two-photon absorption. Since the band-gap frequency is much smaller than twice the laser frequency, the density of states is high in the valence and conduction bands, and a large density of free carriers (on the order of 10^{18} cm^{-3}) can be easily created without any saturation of the two-photon absorption. After intraband relaxation, which occurs in a time smaller than 1 ps, the free carriers accumulate at the bottom of the conduction band (CB) for electrons and at the top of the valence band (VB) for holes. On the other hand, the density of states associated with one-photon transitions for frequencies near the band gap is very low so that a population inversion can be easily obtained as in optically pumped semiconductor lasers.[14]

According to this analysis a strong red emission occurring at ≈ 2 eV was clearly seen for temperatures smaller than 80 K (for higher temperatures population inversion no longer occurs[15]). The signal corresponding to this red emission was detected by using a fast pin photodiode and a 400-MHz bandwidth oscilloscope. The signal consisted of a high unresolved peak (less than 1 ns in duration) and a low-intensity exponential decay with a relaxation time of about 10 ns. This observation evidently proved that the red emission was in fact stimulated. We also verified that, at least for laser intensities less than 1 GW/cm^2, the intensity of the stimulated red emission was proportional to the square of the laser pulse energy showing that the excitation was actually performed by two-photon absorption.

Let us also note that a red spontaneous fluorescence was also observed at 2 eV in Cd-Mn-Te by Moriwaki *et al.* and attributed to the transition $^4T_1 \rightarrow {}^6A_1$ of Mn^{2+} ions.[16] However, as this transition is one-photon forbidden for a free ion, the corresponding transition moment could be too small even in the crystal to allow stimulated emission. Moreover, the fast spontaneous relaxation ($\tau = 10$ ns) also observed is not very probable for the Mn^{2+} ion transition [$\tau \approx 10$ μs at 4 K (Ref. 17)] so that the red emission observed in our experiment is most likely due to stimulated interband recombination.

V. MAGNETIC-FIELD DEPENDENCE OF PIFR

A. Experimental results

The dependence of the light-induced Faraday rotation angle θ_{NL} versus the applied magnetic-field intensity up to 4 T is shown in Fig. 4; the sample temperature was 10 K and the laser peak intensity about 1 GW/cm^2. As seen there for low magnetic fields, less than $H_v = 0.5$ T in our sample, the relative photoinduced change of the Faraday rotation amounted to 14%, while for magnetic fields

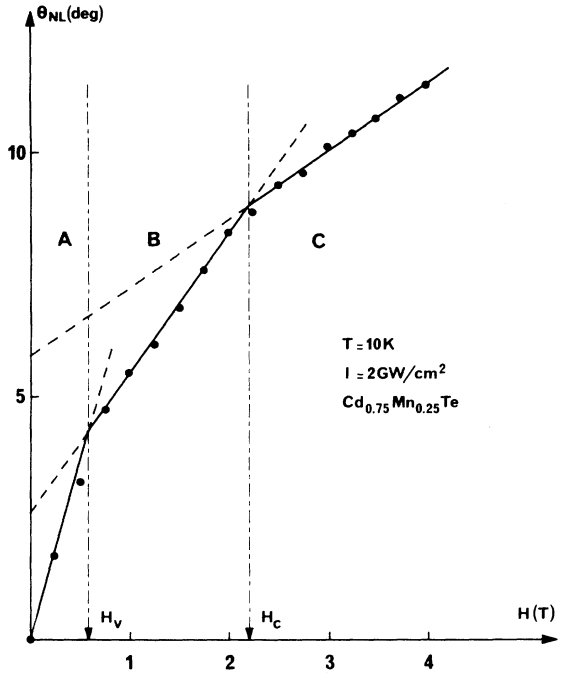

FIG. 4. Nonlinear Faraday rotation as a function of the applied magnetic field. H_v and H_c are the values of H limiting regions (A), (B), and (C) (see text).

larger than $H_c=2.25$ T this amounted to only 6%, implying that saturation set in at different stages as the magnetic field increased. The results actually could be fitted with three straight lines of decreasing slopes as the magnetic-field intensity increased.

B. Theory

The saturation of the photoinduced Faraday rotation with increasing values of the magnetic field can be related to the mechanisms that are responsible for the photoinduced Faraday effect and, by the same token, can be used to extract information concerning them. We point out here that, in our study, the laser frequency is far from one- or two-photon resonance with bound excitons, and in contrast to the case of Ref. 29, the role played by bound magnetic polarons in the optically induced Faraday effect is not important here.

1. General expression of the Faraday rotation angle

In the Faraday configuration in which the magnetic field **H** is applied along the propagation direction of the electromagnetic wave of frequency ω, the Faraday rotation angle θ_F for an optically isotropic medium of thickness ℓ is given by

$$\theta_F=\frac{\omega\ell}{2c}(\tilde{n}_- -\tilde{n}_+) . \tag{4}$$

In Eq. (4), c is the light velocity in vacuum and $\tilde{n}_\mp$ are the effective refractive indices for the two counterrotating circular polarization $\tilde{\sigma}_\mp$. At moderately high laser intensities I these can be written in the form

$$\tilde{n}^{\,2}_\mp=1+4\pi\left[\chi^{(1)}+\Delta\chi^{(1)}_\mp+\chi^{(3)}+\Delta\chi^{(3)}_\mp I\right] , \tag{5}$$

where $\chi^{(1)}$ is the linear susceptibility at $H=0$ which in our case is real, since the relevant frequency ω is well below the onset of real one-photon transitions, and $\chi^{(3)}$ is the third-order susceptibility $\chi^{(3)}(\omega,-\omega,\omega)$ which enters the optical Kerr effect coefficient n_2. $\Delta\chi^{(1)}_\mp$ and $\Delta\chi^{(3)}_\mp$ are the modifications of the above coefficients, $\chi^{(1)}$ and $\chi^{(3)}$, respectively, induced by the magnetic field. Accordingly, the Faraday rotation is

$$\theta_F=\frac{\pi\omega l}{n_0 c}\left[\left[\Delta\chi^{(1)}_- -\Delta\chi^{(1)}_+\right]+\left[\Delta\chi^{(3)}_- -\Delta\chi^{(3)}_+\right]I\right] , \tag{6}$$

where n_0 is the refractive index of the DMS sample at frequency ω.

2. Intraband relaxation

Calculation of θ_F would require the use of the density-matrix approach to susceptibilities[18] in the case of a semiconductor system. Such a calculation is quite difficult and can be avoided in a first step if we look carefully at the intraband relaxation process. Indeed, carriers are created in the conduction and valence bands through two-photon absorption with an energy excess of about 0.4 eV which is distributed into the CB and VB according to the ratio of the effective masses m_v and m_c. The carriers relax through collisions between them and with optical phonons in a time span (<1 ps) which is much less than the pulse duration.[19] However, as optical phonons have frequencies of the order of 150 cm^{-1}, a quasiequilibrium is set in the bands at a temperature which can be higher than that of the lattice.[20] Such an observation is reported in the case of Cd-Te for 30 ps duration Nd-YAG laser pulses,[21] a situation which is quite comparable to ours. Moreover, the quasiequilibrium temperatures can be different in the valence band (T_v) and in the conduction band (T_c) with the restriction $T_v \le T_c$.[19]

3. The equivalent system

As the quasiequilibrium is reached in a time span much smaller than the pulse duration, it is possible to use an equivalent two-level system to describe the susceptibilities.[22] However, as a magnetic field is applied to the medium, Zeeman effect splits the $J=\frac{3}{2}$ valence level and the $J=\frac{1}{2}$ conduction level into four and two sublevels, respectively (see Fig. 5). Such a model was already successfully used to analyze the linear Faraday rotation DMS.[7] In Fig. 5, $\Delta E_c=E_{c,1/2}-E_{c,-1/2}$ and $\Delta E_v=E_{v,-3/2}-E_{v,3/2}$ are the Zeeman splittings induced in the presence of the magnetic field. However, in DMS with large Mn^{2+} concentration, these Zeeman splittings are chiefly due to the exchange interaction existing with that of d electrons of the Mn^{2+} ions.[23]

The spin-exchange interaction is described by the Hamiltonian

$$H_{\rm ex}=\mathcal{J}\mathbf{s}\cdot\mathbf{S}=\mathcal{J}(s_z S_z+s_+S_-+s_-S_+) , \tag{7}$$

where **s** and **S** are band-electron and localized-impurity

spin operators, respectively, and $\mathcal{J}$ is the exchange integral which in our case of cubic symmetry (zinc-blende structure) is characterized by two matrix elements $\alpha=\langle s|\mathcal{J}|s\rangle$ and $\beta=\langle p_z|\mathcal{J}|p_z\rangle$ for the conduction and valence bands, respectively.[6]

In such a case ΔE_c and ΔE_v can be written

$$\Delta E_c=\frac{6\alpha M}{g_{\mathrm{Mn}}\mu_B}\ , \tag{8a}$$

$$\Delta E_v=-\frac{6\beta M}{g_{\mathrm{Mn}}\mu_B}\ . \tag{8b}$$

4. *Expressions of $\chi_{\mp}^{(1)}$ and $\chi_{\mp}^{(3)}$*

As the CB and VB are in quasiequilibrium in a time span which is much less than the pulse duration, it is possible to give a time-dependent expression for the susceptibilities, the populations which enter into these susceptibilities also being time dependent.

The linear susceptibility is calculated through the density-matrix technique[18] applied to our six-level system. Taking into account the fact that the $|v,-\frac{1}{2}\rangle\rightarrow|c,+\frac{1}{2}\rangle$ and $|v,\frac{1}{2}\rangle\rightarrow|c,-\frac{1}{2}\rangle$ transitions are three times less probable than that occurring between $|v,-\frac{3}{2}\rangle\rightarrow|c,-\frac{1}{2}\rangle$ and $|v,\frac{3}{2}\rangle\rightarrow|c,+\frac{1}{2}\rangle$ levels,[6] the susceptibilities $\chi_{\mp}^{(1)}$ are given by

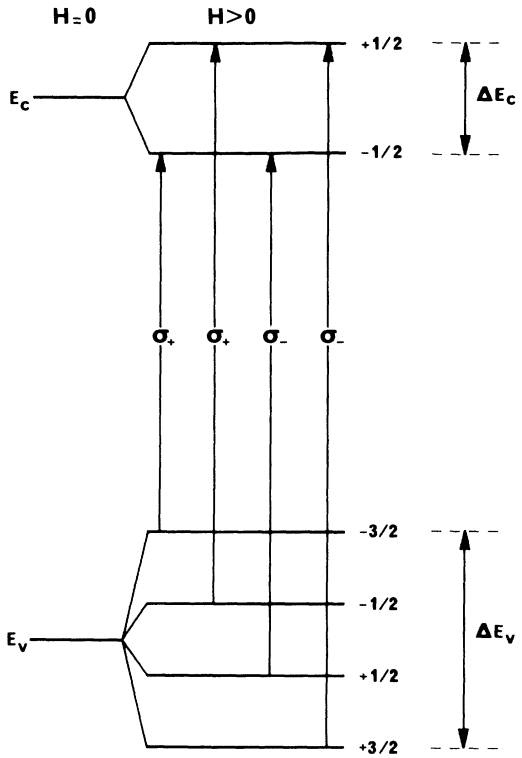

FIG. 5. The equivalent system used for the calculation of the photoinduced Faraday rotation angle.

$$\chi_{\mp}^{(1)}(t,I)=\frac{2}{3}\mathcal{N}_0 d_{\mp}^2\left[3(\rho_{c,\pm1/2}^{(t)}-\rho_{v,\pm3/2}^{(t)})\frac{(E_{c,\pm1/2}-E_{v,\pm3/2})}{(\hbar\omega)^2-(E_{c,\pm1/2}-E_{v,\pm3/2})^2}\right.$$
$$\left.+(\rho_{c,\mp1/2}^{(t)}-\rho_{v,\pm1/2}^{(t)})\frac{(E_{c,\mp1/2}-E_{v,\pm1/2})}{(\hbar\omega)^2-(E_{c,\mp1/2}-E_{v,\pm1/2})^2}\right]\ , \tag{9}$$

where $\mathcal{N}_0$ is the population density of the equivalent two-level system[22] and $d_{\mp}$ are the electric dipolar transition moments for the counterrotating polarizations $\sigma_{\mp}$. In Eq. (9), $\rho_{c,\pm1/2}^{(t)}$ and $\rho_{v,\pm x/2}^{(t)}$ $(x=1,3)$ are the probability for an electron to occupy the $|c,\pm\frac{1}{2}\rangle$ and $|v,\pm x/2\rangle$ levels, respectively. For a low laser intensity, the VB is entirely filled and the CB is empty so that $\rho_{c,\mp1/2}^{(t)}=0$ and $\rho_{v,\pm x/2}^{(t)}=\frac{1}{4}$ $(x=1,3)$. On the other hand, at high laser intensity $I(t)$ large electron and hole densities $\Delta n_c(t)$ are created by two-photon absorption. However, as discussed in Sec. IV, due to stimulated recombination, the densities of thermalized carriers $\Delta n_T(t)$ can be strongly less than $\Delta n_c(t)$. Although a complete calculation is necessary to take this stimulated recombination into account, as a first step we may set $\Delta n_T(t)=q\Delta n_c(t)$ where q is a phenomenological parameter $(q<1)$. The population factors of Eq. (9) are then

$$\mathcal{N}_0\rho_{c,\pm1/2}=\Delta n_T(t)f_c(\pm1/2)\ , \tag{10a}$$

$$\mathcal{N}_0\rho_{v,\pm x/2}=\frac{\mathcal{N}_0}{4}-\Delta n_T(t)f_v\left[\pm\frac{x}{2}\right]\quad(x=1,3)\ , \tag{10b}$$

where $f_c(\pm\frac{1}{2})$ and $f_v(\pm x/2)$ are the statistical repartition functions of electrons in CB and holes in VB, respectively.

If the carrier density is high the Fermi-Dirac statistics apply, while the Maxwell-Boltzmann statistics are a correct approximation for low carrier density. As in our case the stimulated recombination hinders the increase with time of the carrier density, the Maxwell-Boltzmann statistics can apply so that

$$f_c(\pm\tfrac{1}{2})=\frac{\exp\left[\mp\dfrac{\Delta E_c}{2kT_c}\right]}{\exp\left[\dfrac{\Delta E_c}{2kT_c}\right]+\exp\left[-\dfrac{\Delta E_c}{2kT_c}\right]}\ , \tag{11a}$$

$$f_v(\pm x/2)=\frac{\exp\left[\mp\dfrac{\Delta E_v}{2xkT_v}\right]}{\exp\left[\dfrac{\Delta E_v}{2kT_v}\right]+\exp\left[\dfrac{\Delta E_v}{6kT_v}\right]+\exp\left[-\dfrac{\Delta E_v}{6kT_v}\right]+\exp\left[-\dfrac{\Delta E_v}{2kT_v}\right]} \quad (x=1,3) . \tag{11b}$$

Equations (10) and (11) must be included into Eq. (9) to get the expression of $\chi_{\mp}^{(1)}(t)$.

On the other hand, as two-photon transitions are involved in the calculation of $\chi_{\mp}^{(3)}$ through the density-matrix technique, our equivalent system is not relevant. Therefore, the same phenomenological value as in Ref. 8 is taken to express $\chi_{\mp}^{(3)}I$, namely, $A_{\pm}IM_0$, where $A_{\pm}$ is a factor which depends on the laser frequency but is independent of the laser intensity and magnetization.

5. *The three contributions to the photoinduced Faraday rotation angle*

The Faraday rotation angle defined by Eq. (6) can be easily calculated using Eqs. (8) through (11). If the oscillator strength is assumed to be magnetic-field independent[7] θ_F can be set in the following form:

$$\theta_F=\frac{\pi\omega\mathcal{L}}{n_0c}\{-\tfrac{2}{3}\mathcal{N}_0d^2F^2(\tfrac{5}{3}\Delta E_v+2\Delta E_c) +\tfrac{2}{3}\Delta n_T(t)d^2F[3B_{3/2}(\eta_v)+2B_{1/2}(\eta_c)] +\Delta A\, IM_0\} \tag{12}$$

with $F=E_g/[Eg^2-(\hbar\omega)^2]$, $\Delta A=A_- - A_+$, and $\eta_y=\Delta E_y/2kT_y$ $(y=c,v)$. In Eq. (12), Eg is the semiconductor band-gap energy, d the unperturbed dipolar transition moment, and $B_{x/2}(\eta_y)$ the Brillouin function for electrons in CB ($x=1$ and $y=c$) and holes in VB ($x=3$ and $y=v$).

We stress the fact that the effective magnetization M involved in the expression of ΔE_y $(y=c,v)$ in Eqs. (8) and (12) consists of the magnetization M_0 due to the applied magnetic field H and, as will be demonstrated in the next section, a term ΔM induced by the spin flip-flop of photocarriers. As a consequence, besides the linear Faraday rotation angle

$$\theta_L=-\frac{2\pi\omega\mathcal{L}}{3n_0c}\mathcal{N}_0d^2F^2\left[\alpha-\frac{5\beta}{3}\right]\frac{M_0}{g_{\mathrm{Mn}}\mu_B} , \tag{13}$$

we write the photoinduced Faraday rotation angle

$$\theta_{\mathrm{NL}}=\theta_K+\theta_p+\theta_M \tag{14}$$

with the three contributions

$$\theta_K=\frac{\pi\omega\mathcal{L}}{n_0c}\Delta A\, IM_0 , \tag{15a}$$

$$\theta_p=\frac{\pi\omega\mathcal{L}}{n_0c}\tfrac{2}{3}\Delta n_T(t)d^2F[3B_{3/2}(\eta_v)+2B_{1/2}(\eta_c)] , \tag{15b}$$

$$\theta_M=-\frac{\pi\omega\mathcal{L}}{n_0c}\tfrac{2}{3}\mathcal{N}_0d^2F^2\left[\alpha-\frac{5\beta}{3}\right]\frac{\Delta M}{g_{\mathrm{Mn}}\mu_B} . \tag{15c}$$

The first contribution θ_K given by Eq. (15a) is due to the Kerr effect in the presence of the magnetic field; this contribution only was taken into account in Ref. 8. The second term θ_p [see Eq. (15b)] corresponds to a nonlinear rotation induced by carrier density changes and the last one, θ_M in Eq. (15c) shows the importance of the magnetization change of Mn^{2+} ions.

6. *The photoinduced magnetization*

Let us assume that electrons and holes are created through two-photon absorption with equal densities of spin up and spin down states irrespective of the excitation polarization; this assumption is, in fact, corroborated experimentally by the observation of equal amounts of absorption for linearly and circularly (right and left) polarized beams. At the intraband quasiequilibrium which is reached in less than 1 ps, the spin populations are no more degenerate; this implies that the photocarrier spins do change during the intraband relaxation process by a fast mechanism. Among the possible mechanisms (electron-electron, electron-hole, electron-phonon, etc.)[24] the spin-exchange interaction, which can induce fast flip-flop processes through the transverse part $s_+S_-+s_-S_+$ of the exchange Hamiltonian H_{ex}, plays an important role.[25] This mechanism, which was studied theoretically[26,27] has a relaxation time of the order of 1 ps (Refs. 28–30) in contrast to the much slower relaxation process related to the s_zS_z term ($\tau>1$ μs) (Ref. 31) and whose effect can be safely neglected here. The operator $s_+S_-+s_-S_+$ does not modify the total angular momentum, so that one has

$$xN_0\langle S_0\rangle+\Delta n_c(t)[p_c\langle s_e^c\rangle+p_v\langle s_h^c\rangle] =xN_0\langle S_T\rangle+\Delta n_c(t)[p_c\langle s_e^T\rangle+p_v\langle s_h^T\rangle] , \tag{16}$$

where $\langle S_0\rangle=-\frac{5}{2}B_{5/2}[5\ g_{\mathrm{Mn}}\mu_BH/(2kT)]$ is the average spin per Mn^{2+} site, $\langle s_e^c\rangle$ and $\langle s_h^c\rangle$ are the average spins per electron and hole at the moment of their generation by two-photon absorption, and p_c and p_v are the probability for electron and hole spin relaxation through spin exchange, respectively. Since these carriers are created with equal amounts of spin up and down states, one has $\langle s_e^c\rangle=\langle s_h^c\rangle=0$. In Eq. (16), $\langle S_T\rangle=\langle S_0\rangle+\langle\Delta S\rangle$ is the average spin per Mn^{2+} site after the intraband relaxation, $\langle\Delta S\rangle$ being its photoinduced variation; $\langle s_e^T\rangle$ and $\langle s_h^T\rangle$ are the average spin per electron and hole at quasiequilibrium so that

$$\langle s_e^T\rangle=-\tfrac{1}{2}B_{1/2}(\eta_c) , \tag{17a}$$

$$\langle s_h^T\rangle=-\tfrac{3}{2}B_{3/2}(\eta_v) . \tag{17b}$$

Using Eqs. (16) and (17), the spin-flip-flop-induced

magnetization of Mn^{2+} ions $\Delta M=-xN_0\, g_{Mn}\mu_B\langle\Delta S\rangle$ becomes

$$\Delta M=-\tfrac{1}{2}\Delta n_c(t)g_{Mn}\mu_B[p_cB_{1/2}(\eta_c)+3p_vB_{3/2}(\eta_v)]\ . \quad (18)$$

As shown by Eq. (18), the photoinduced magnetization is proportional to the density of *created* photocarriers and depends on the magnetic field and temperature through the same Brillouin functions as does the population contribution of the photoinduced Faraday rotation.

C. Discussion

By comparing the experimental results of Fig. 4 to the calculations of Sec. V B, it is possible to verify our theoretical approach and to extract some information about the nonlinear Faraday process.

1. Qualitative agreement

It is not our intention to use the previous model here to get a quantitative fit between theory and experiment. However, a qualitative agreement can be easily seen; indeed, the Brillouin function $B_J(\eta_y)$ can be reduced, to a good approximation, to two straight lines of equations $B_J(\eta_y)=(J+1)\eta_y/(3J)$ and $B_j(\eta_y)=1$ for small and large values of η_y, respectively. In these expressions, $J=\frac{3}{2}$ and $y=v$ and $J=\frac{1}{2}$ and $y=c$ for the valence and conduction bands, respectively.

Since $-\alpha<\beta$, or $\eta_c<\eta_v$, $B_{3/2}(\eta_v)$ saturates before $B_{1/2}(\eta_c)$ when the magnetization is increased. For small values of H both $B_{3/2}(\eta_v)$ and $B_{1/2}(\eta_c)$ are proportional to M so that θ_{NL} is given by

$$\theta_{NL}=[\lambda_k I+(\lambda_{PM}^{(c)}+\lambda_{PM}^{(v)})\Delta n_c(t)]M_0\ . \quad (19)$$

In Eq. (19), $\lambda_k=\pi\omega l\Delta A/n_0c$ is related to the Kerr contribution and $\lambda_{PM}^{(c)}$ and $\lambda_{PM}^{(v)}$ are connected to the population and magnetic flip-flop processes for the conduction electrons and valence holes, respectively. Note that the constants $\lambda_{PM}^{(c)}$ and $\lambda_{PM}^{(v)}$, which can be easily calculated owing to Eqs. (15)–(18), are independent on the laser intensity and applied magnetic field. As the magnetization is proportional to the magnetic field (see Sec. III), θ_{NL} is proportional to H; this corresponds to zone A in Fig. 4.

As H increases beyond a value H_v such that $\eta_v=\frac{9}{5}$, $B_{3/2}(\eta_v)$ saturates at the value one while $B_{1/2}(\eta_c)$ is still proportional to η_c and θ_{NL} becomes

$$\theta_{NL}=[\lambda_k I+\lambda_{PM}^{(c)}\Delta n_c(t)]M_0-\frac{9\, g_{Mn}\mu_B kT_v}{5\beta}\lambda_{PM}^{(v)}\Delta n_c(t)\ . \quad (20)$$

As a consequence, the photoinduced Faraday rotation exhibits a linear dependence versus the applied magnetic field with a smaller slope than that given by Eq. (19); this is zone B of Fig. 4.

Finally, beyond a value H_c such that $\eta_c=1$, $B_{1/2}(\eta_c)$ also saturates at the value one and

$$\theta_{NL}=\lambda_k IM_0+g_{Mn}\mu_B k\left[\frac{T_c\lambda_{PM}^{(c)}}{\alpha}-\frac{9T_v\lambda_{PM}^{(v)}}{5\beta}\right]\Delta n_c(t)\ . \quad (21)$$

The photoinduced Faraday rotation has, then, a linear dependence versus H and the slope is only due to the Kerr contribution; this corresponds to zone C in Fig. 4.

2. Determination of the quasiequilibrium temperatures

The quasiequilibrium temperatures in the CB and VB can be easily determined by using the intersection of the two asymptotic straight lines $B_J(\eta_y)=(J+1)\eta_y/(3J)$ and $B_J(\eta_y)=1$ of the Brillouin function. As a consequence, the angular points of Fig. 4 are obtained for

$$\frac{J+1}{J}\frac{\Delta E_y}{6kT_y}=1\ . \quad (22)$$

The exciton Zeeman splittings ΔE_y $(y=c,v)$ were measured by Gaj, Ginter, and Galazka in $Cd_{0.80}Mn_{.20}Te$, a composition which is close to ours.[6] Using their determination and doing corrections for the magnetic-field value and for the temperature by using Fig. 2, one finds $T_c=59$ K and $T_v=35$ K. As predicted in Sec. V B 2, these values are somewhat higher than the 10 K of the lattice.

3. Intensity dependence of the PIFR

As the carriers are created through two-photon absorption their density, $\Delta n_c(t)$ is proportional to the

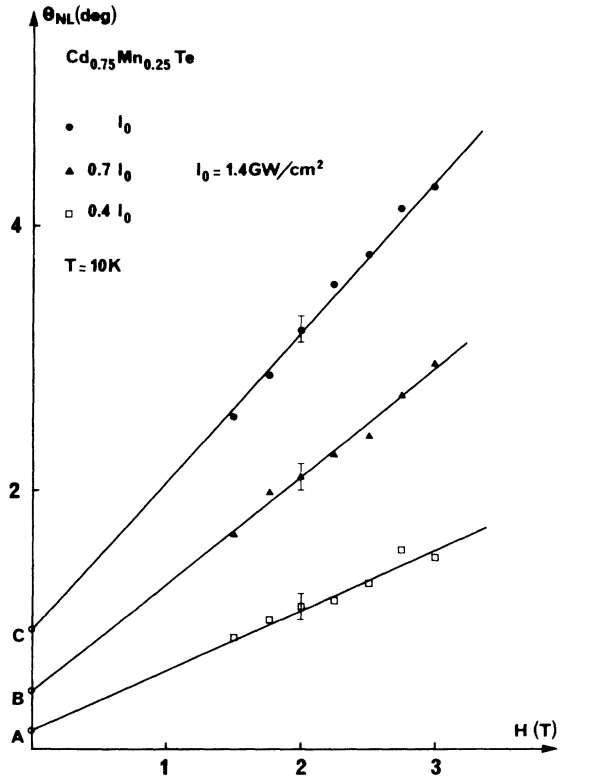

FIG. 6. Nonlinear Faraday rotation as a function of the applied magnetic field for different values of the laser intensity (I_0; 0.7 I_0; 0.4 I_0). The slopes of the fits are m_0, $0.73m_0$, and $0.41m_0$. The intercepts of the θ_{NL} axis are: θ_0, $(0.74)^2\theta_0$, and $(0.41)^2\theta_0$.

square of the laser intensity. Consequently, the population and magnetic flip-flop contributions of the photoinduced Faraday rotation angle are proportional to I^2. If the laser intensity is not too high ($I < 1.5$ GW/cm^2), as observed experimentally, the population and magnetic contributions of conduction electrons $\lambda_{PM}^{(c)} \Delta n_c(t)$ can be neglected with respect to the Kerr contribution $\lambda_k I$, and Eq. (20) reduces to

$$\theta_{NL} = \lambda_k I M_0 - \frac{9\, g_{\mathrm{Mn}} \mu_B k T_v}{5\beta} \lambda_{PM}^{(v)} \Delta n_c(t) \ . \tag{23}$$

The slope and intercept of the θ_{NL} axis of the straight line giving the evolution of θ_{NL} with respect to H as given by Eq. (23) must, therefore, exhibit different evolutions as the laser intensity is increased. This behavior was confirmed experimentally, as proven in Fig. 6 where θ_{NL} is plotted versus H for three different laser intensities ($I_L = 1.4$, 1.0, and 0.56 MW/cm^2). Indeed, the slope of the straight lines, which are the fits to the experimental results, are actually proportional to the laser intensity and, although the precision is not as good in this case, the intercepts (A,B,C in Fig. 6) are found to be proportional to I^2. Evidently, such an agreement with the predictions of Eq. (23) is a supplementary proof of the validity of our analysis.

VI. TEMPERATURE DEPENDENCE OF PIFR

In the photoinduced Faraday rotation angle given in Eq. (15), several parameters depend on the temperature:

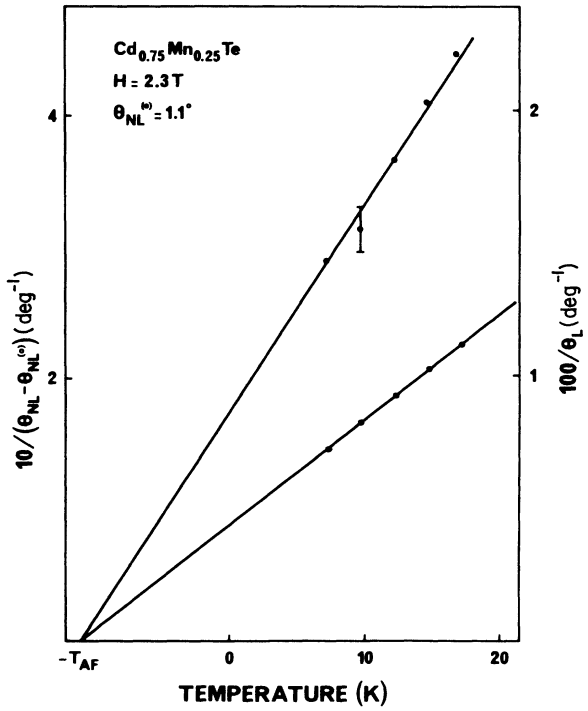

FIG. 7. Inverse of the Kerr contribution to the photoinduced Faraday rotation angle $\{[\theta_{NL}-\theta_{NL}(0)]^{-1}\}$ together with the inverse of the linear Faraday rotation angle ($\theta_L{}^{-1}$) as a function of the temperature. The antiferromagnetic temperature T_{AF} is the same for both fits.

the band gap E_g, the Brillouin functions $B_J(\eta_y)$ which determine the population repartitions of electrons and holes in the CB and VB and the magnetization M_0 of Mn^{2+} ions (see Sec. III). However, in the 5–20-K range of our experimental investigation, the band gap is almost temperature independent,[32] and for a sufficiently high magnetic field the Brillouin functions are saturated so that the temperature dependence of θ_{NL} is reduced to that of the M_0 already discussed in Sec. III.

As shown in Sec. V C 3, when the laser intensity is not too high the photoinduced Faraday rotation angle is given by Eq. (23) which involves the Kerr contribution for the slope and the hole-induced population and magnetic contribution for the intercept. As a consequence, as verified experimentally for three different temperatures ($T = 10$, 12.5, and 17.5 K) the slope depends on T while the intercept $\theta_{NL}(0)$ is the same for the three temperatures tested. This result can be used to verify that the Kerr contribution to θ_{NL} has the same temperature dependence as θ_L. Indeed, as shown in Fig. 7, the inverse of θ_{NL}-$\theta_{NL}(0)$ exhibits a linear growth with respect to T, as it is in the case for $\theta_L{}^{-1}$ also plotted in the same figure. Moreover, it can be seen from Fig. 7 that the same antiferromagnetic temperature $T_{AF} = 10.5$ K is involved in both measurements. This confirms that the temperature dependence of the photoinduced Faraday rotation is mainly related to that of the magnetization of Mn^{2+} ions.

VII. CONCLUSION

An experimental investigation of the Faraday rotation process has been performed in the diluted magnetic semiconductor Cd-Mn-Te through the dependence of the Faraday rotation angle with respect to magnetic field, laser intensity, and temperature changes.

At low laser intensity, the measurement of the traditional Faraday rotation angle has shown that the antiferromagnetic temperature and effective concentration introduced in the expression of the magnetization of Mn^{2+} ions depends linearly on the magnetic field, indicating that the coupling between Mn^{2+} ions could be more efficient at larger magnetic fields.

At high laser intensity, the determination of the photoinduced Faraday rotation variation has allowed the identification of three contributions which have been estimated theoretically: a fast Kerr contribution proportional to the laser intensity, a population change contribution through two-photon absorption and stimulated recombination of photoinduced carriers, and a much slower one due to the exchange interaction existing between the spins of the s and p photoinduced carriers and that of the d electrons of Mn^{2+} ions. The population and magnetic contribution, whose amplitude was measured to be quadratic in the laser intensity, have been demonstrated to saturate as the magnetic field increases. The thresholds have been attributed to the saturation of the total spin of holes and electrons in the valence and conduction bands, respectively. An experimental study of the temperature dependence of the photoinduced Faraday rotation angle below 20 K has also proven that, as expected

theoretically, the population and magnetic contributions were independent of the temperature while the Kerr term exhibited the same behavior as the linear Faraday rotation angle. Evidently, similar experiments should be performed for different Mn^{2+} ion concentrations, in particular, for low x values when there is no need for the effective concentration, a situation which would certainly improve the interpretation of the data. Such experiments will be undertaken as soon as such samples are available.

Moreover, time-resolved experiments would be very useful to better characterize this nonlinear effect. Pump and probe experiments are presently going on and preliminary results confirm our analysis; all the results concerning this time-resolved study will be published elsewhere.

We wish to point out also that the study of the photoinduced Faraday effect may provide very valuable information about these processes and, in addition, could lead to applications such as optically addressed optical valves or for generating large instantaneous Mn^{2+} ion magnetization and spin alignment, processes which are not possible by direct application of magnetic-field pulses.

ACKNOWLEDGMENTS

We thank Dr. R. Triboulet from the Laboratoire de Physique des Solides, Centre National de la Recherche Scientifique, in Meudon, for providing very good quality $Cd_{1-x}Mn_xTe$ samples.

[1]See, for instance, Y. R. Shen, *The Principles of Nonlinear Optics* (Wiley, New York, 1984).

[2]I.O.G. Davies, P.E.G. Barid, and J-L. Nicol, J. Phys. B **20**, 5371 (1987).

[3]K. H. Drake, W. Lange, an J. Mlynek, Opt. Commun. **66**, 315 (1988).

[4]X. Chen, V. L. Telegdi, and A. Weiss, Opt. Commun. **74**, 301 (1990).

[5]K. Kubota, J. Phys. Soc. Jpn. **29**, 998 (1970).

[6]J. A. Gaj, J. Ginter, and R. R. Galazka, Phys. Status Solidi B **89**, 655 (1978).

[7]D. U. Bartholomew, J. K. Furdyna, and A. K. Ramdas, Phys. Rev. B **34**, 6934 (1986).

[8]J. Frey, R. Frey, C. Flytzanis, and R. Triboulet, Opt. Commun. **84**, 76 (1991).

[9]J. Frey, R. Frey, C. Flytzanis, and R. Triboulet J. Opt. Soc. Am. B (to be published).

[10]J. A. Gaj, R. R. Galazka, and M. Nawrocki, Solid State Commun. **25**, 193 (1978).

[11]A. V. Komarov, S. M.. Ryabchenko, O. V. Terletskii, I. I. Zheru, and R. D. Ivanckuk, Zh. Eksp. Teor. Fiz. **73**, 608 (1977) [Sov. Phys. JETP **46**, 318 (1977)].

[12]J. A. Gaj, R. Planel, and G. Fishman, Solid State Commun. **29**, 435 (1979).

[13]E. Kierzek-Pecold, W. Szymanska, and R. R. Galazka, Solid State Commun. **50**, 685 (1984).

[14]H. Kressel, in *Laser Handbook*, edited by F. T. Arecchi and E. O. Schulz-Dubois (North-Holland, Amsterdam, 1972), Vol. 1, p. 446.

[15]G. P. Agrawal and N. K. Dutta, *Long Wavelength Semiconductor Lasers*, (Van Nostrand Rheinhold, New York, 1986), p. 128.

[16]M. Moriwaki, R. Y. Tao, R. R. Galazka, W. M. Becker, and J. Richardson, Physica, **117B**, 467 (1983).

[17]O. Goede and Dang Dinh Thong, Phys. Status Solidi B **124**, 343 (1984).

[18]C. Flytzanis, in *Quantum Electronics*, edited by H. Rabin and C. L. Tang (Academic, New York, 1975), Vol. 1, Part A.

[24]E. J. Johnson, R. J. Seymour, and R. R. Alfano, in *Semiconductors Probed by Ultrafast Laser Spectroscopy*, edited by R. R. Alfano (Academic, New York, 1984), Vol. II, p. 200.

[20]S. A. Lyon, J. Lumin. **35**, 121 (1986).

[21]J. Collet, A. Cornet, M. Pugnet, and T. Amand, Solid State Commun. **42**, 883 (1982).

[22]F. de Rougemont and R. Frey, Phys. Rev. B **37**, 1237 (1988).

[23]J. K. Furdyna, J. Appl. Phys. **64**, R29 (1988).

[24]E. J. Johnson, R. J. Seymour, and R. R. Alfano, in *Semiconductors Probed by Ultrafast Laser Spectroscopy*, edited by R. R. Alfano (Academic , New York, 1984), Vol. II, p. 200.

[25]S. M. Ryabchenko, Yu. G. Semenov, O. V. Terletskii, Zh. Eksp. Teor. Fiz. **82**, 951 (1982) [Sov. Phys. JETP **55**, 557 (1982)].

[26]H. Krenn, K. Kaltenegger, and G. Bauer, Solid State Electron. **31**, 481 (1988).

[27]G. Bastard and L. L. Chang, Phys. Rev. B **41**, 7899 (1990).

[28]H. Krenn, W. Zawadzki, and G. Bauer, Phys. Rev. Lett. **55**, 1510 (1985).

[29]D. D. Awschalom, J-M. Halbout, S. von Molnar, T. Siegrist, and F. Holtzberg, Phys. Rev. Lett. **55**, 1128 (1985).

[30]D. D. Awschalom and J. M. Halbout, J. Magn. Magn. Mater. **54–57**, 1381 (1986).

[31]D. Scalbert, J. Cernogora, and C. Benoit à la Guillaume, Solid State Commun. **66**, 571 (1988).

[32]Y. R. Lee and A. K. Ramdas, Solid State Commun. **51**, 861 (1984).